


 Cite this: *RSC Adv.*, 2020, 10, 21222

# Development of glycine-copper(II) hydroxide nanoparticles with improved biosafety for sustainable plant disease management

 Hongqiang Dong,<sup>ab</sup> Renci Xiong,<sup>b</sup> You Liang,<sup>a</sup> Gang Tang,<sup>a</sup> Jiale Yang,<sup>a</sup> Jingyue Tang,<sup>a</sup> Junfan Niu,<sup>a</sup> Yunhao Gao,<sup>a</sup> Zhiyuan Zhou<sup>a</sup> and Yongsong Cao<sup>id\*</sup>

Cabbage black rot caused by *Xanthomonas campestris* pv. *campestris* (Xcc) leads to decrease of the production of up to 70%. Copper biocides are widely used to control this disease because of their low-cost application and broad-spectrum antimicrobial activities. Extensive spraying of traditional copper biocides would cause undesirable effects on plants and the environment. In this work, a novel copper-based microbicide was prepared by binding copper with glycine in sodium hydroxide solution (Gly-Cu(OH)<sub>2</sub> NPs) and characterized by inductively coupled plasma atomic emission spectroscopy, high-resolution transmission electron microscopy, Fourier transformation infrared spectroscopy, and dynamic light scattering. The results showed that the prepared Gly-Cu(OH)<sub>2</sub> NPs had a mean diameter of 240 nm with copper content more than 25.0% and their antimicrobial efficacies against Xcc were significantly better than Kocide 3000 at 400–800 mg L<sup>-1</sup> of copper after spraying for 14 days. The phytotoxicity tests under greenhouse conditions showed that Gly-Cu(OH)<sub>2</sub> NPs were safer to plants than Kocide 3000 and obviously promoted the growth of plants, which led to the increase of fresh weights of Chinese cabbage and tomato seedlings by 6.34% and 3.88% respectively at a concentration of 800 mg L<sup>-1</sup> of copper. As a novel copper-based microbicide, the Gly-Cu(OH)<sub>2</sub> NPs can improve effective utilization of copper-based bactericides and reduce phytotoxicity to plants and would be a potential alternative for sustainable plant disease management.

Received 4th March 2020

Accepted 21st May 2020

DOI: 10.1039/d0ra02050h

[rsc.li/rsc-advances](http://rsc.li/rsc-advances)

## Introduction

Black rot, caused by *Xanthomonas campestris* pv. *campestris* (Xcc), is a major disease of brassica crops, which leads to Chinese cabbage necrotic leaf lesions and defoliation.<sup>1,2</sup> Once a field becomes infested with this bacterial spot, it is extremely difficult to have success in disease control.<sup>3</sup> For these reasons, numerous control measures including biological control and chemical control were proposed to protect Chinese cabbages from black rot.<sup>4</sup> Although streptomycin was the dominant bactericide used to manage black rot, antagonistic bacteria became the ideal choice for biological control because of the emergence of streptomycin-resistant xanthomonas.<sup>5,6</sup> It is reported that antagonistic bacteria including *Bacillus* sp., *Pseudomonas* sp. were used as an effective method to control black rot disease in brassica crops.<sup>7,8</sup> However, ensuring the satisfactory efficacy of antagonistic bacteria in the field conditions is a great challenge because of high economic cost and the harsh environmental requirements for their proliferation.<sup>9,10</sup> At

present, copper biocides are regarded as the most frequently used agents for control of black rot in Chinese cabbages because of their broad spectrum, relatively inexpensive price, and fewer instrumental requirements for application than other bactericides.<sup>11,12</sup> Commercially available copper-based bactericides typically contain micron-sized metallic copper in the form of insoluble copper compounds, such as Cu(II) hydroxide, basic Cu(II) sulfate, Cu(II) oxide, thiodiazole copper and Cu(II) oxychloride.<sup>13,14</sup> Kocide 3000 (DuPont, Wilmington, DE), a commercialized copper bactericide, contains metallic copper at approximately 5 μm in the form of copper(II) hydroxide.<sup>15</sup> To enhance lasting antimicrobial activity without obvious plant damage, multiple applications of Cu biocides are necessary in a single growing season.<sup>16</sup> Although copper is an essential element of plant, long-term and frequent applications of copper biocides have resulted in the increase of copper concentration and led to heavy metal pollution in the environment.<sup>17,18</sup> Large dose exposure to copper will lead to a broad range of deleterious effects on plants, such as photosynthetic inhibition and pigment synthesis, damage to plasma membrane and other metabolic disturbance.<sup>19,20</sup> Moreover, excessive copper in the environment can cut down soil respiration, lessen microbial biomass, and do harm to fish.<sup>21,22</sup> In recent years, nano-metallic compounds were applied to control plant diseases caused by

<sup>a</sup>College of Plant Protection, China Agricultural University, Beijing, China. E-mail: caoyong@126.com; caoys@cau.edu.cn; Fax: +86-10-62734302; Tel: +86-10-62734302

<sup>b</sup>College of Plant Science, Tarim University, Alaer, China



pathogenic microorganisms and showed excellent microbicidal activities.<sup>23–25</sup> In particular, copper nanoparticles have attracted researcher attentions due to their lower cost than silver and gold nanoparticles,<sup>26,27</sup> and they were found to be higher antibacterial activities against plant pathogenic bacteria compared to commercial antibiotic streptomycin sulphate.<sup>28,29</sup> However, copper nanoparticles are extremely easy to aggregate and oxidize in the air, which results in a marked decrease of their antibacterial activity in the field of agriculture.<sup>30</sup> To prevent aggregation of copper nanoparticles, copper and amino acid were designed to bond together by coordination bonds for improving overall antimicrobial efficacy of metallic copper particles.<sup>31,32</sup> Copper complexes of amino acids can release copper ions to achieve microbicidal efficacy and provide amino acids as nutrition for plants at the same time, and have shown to be safer to plants than traditional copper based microbicides.<sup>33,34</sup> Therefore, the development of nanometer-sized copper-based microbicide with good water dispersibility would be an excellent choice for the preparation of novel copper biocides.

In this work, a novel copper-based microbicide was prepared by adding sodium hydroxide to the *cis*-bis(glycinato)copper monohydrate solution. The obtained glycine-functionalized copper(II) hydroxide (Gly-Cu(OH)<sub>2</sub>) nanoparticles were characterized by high-resolution transmission electron microscopy (HRTEM), inductively coupled plasma atomic emission spectroscopy analysis (ICP-AES), Fourier transformation infrared (FTIR) spectroscopy, and dynamic light scattering (DLS) analysis to determine morphology, content, size and zeta potential. Meanwhile, the antimicrobial activity and the safety to plant were also investigated.

## Experimental

### Materials

Cupric acetate monohydrate and glycine (Gly) were supplied by Sinopharm Chemical Reagent Beijing Co., Ltd. (Beijing, China). Copper(II) hydroxide (99%, Chengxin Industry CO. LLC, Shanghai, China), Kocide 3000 (46.1 wt%, copper hydroxide) was supplied by DuPont (Wilmington, DE, USA). *Xanthomonas campestris* pv. *campestris* (Xcc) strain was obtained from the College of Plant Science, Tarim University (Alaer, China).

### Synthesis of *cis*-bis(glycinato)copper (*cis*-Cu(Gly)<sub>2</sub>)

Briefly, glycine (0.2 mol) and cupric acetate monohydrate (0.1 mol) were dissolved respectively in 250 mL of water, heated up to 70 °C, and the obtained solutions were mixed. Then, the mixture was quenched with 250 mL of ethanol. After being cooled to 0 °C under ice bath condition, the precipitate was isolated by vacuum filtration. Finally, the sample washed with ethanol three times and dried under high-vacuum.

### Preparation of Gly-Cu(OH)<sub>2</sub> nanoparticles

The preparation of Gly-Cu(OH)<sub>2</sub> nanoparticles was referenced the literature method with slight modifications.<sup>35</sup> Briefly, 0.04 mol of *cis*-Cu(Gly)<sub>2</sub> was dissolved in 100 mL of water under

constant stirring at room temperature for 30 min. Then, 6 mL of sodium hydroxide solution (1.2 mol L<sup>-1</sup>) was added slowly with a 10 mL syringe and continuously stirred for another 20 min. After that, the blue precipitate was collected by centrifugation (10 000 rpm, 8 min) and washed with water and ethanol respectively three times. The Gly-Cu(OH)<sub>2</sub> NPs were obtained after drying under vacuum.

### Characterization

The morphology of the obtained sample was characterized by a Philips TECNAI 10 transmission electron microscope (TEM). Elemental composition was analyzed with a JEOL JEM-2100F HRTEM equipped with an Oxford INCA energy-dispersive X-ray spectroscopy (EDS) device. The different functional groups present in glycine, *cis*-Cu(Gly)<sub>2</sub>, Cu(OH)<sub>2</sub> and Gly-Cu(OH)<sub>2</sub> were carried out employing a Nicolet Avatar-300 FTIR spectrophotometer from Thermo Scientific in the range of 4000–400 cm<sup>-1</sup>. Particle size and zeta potential of Gly-Cu(OH)<sub>2</sub> and Cu(OH)<sub>2</sub> particles were performed by DLS with a Malvern Zetasizer Nano-ZS90 Instrument (Mastersizer 3000, Malvern Instruments Co. UK).

### Antimicrobial assay *in vitro*

Disk diffusion method was used to evaluate the antimicrobial activities of Kocide 3000 and Gly-Cu(OH)<sub>2</sub> NPs.<sup>36</sup> Firstly, the Xcc strains were incubated for 2 h at 28 °C in a Luria-Bertani (LB) broth and then shaken 150 rpm overnight. The obtained bacteria suspension was diluted to an optical density at 600 nm (OD<sub>600</sub>) of 0.1 (approximately 1 × 10<sup>8</sup> CFU mL<sup>-1</sup>), and 100 μL of this bacterial suspension was spread uniformly on LB agar plates. The small piece of filter papers (6 mm) containing glycine (400 mg L<sup>-1</sup>), Kocide 3000 (0, 25, 50, 100, 200, 400 mg L<sup>-1</sup> of copper), Gly-Cu(OH)<sub>2</sub> NPs (0, 25, 50, 100, 200, 400 mg L<sup>-1</sup> of copper), and sterilize distilled water were placed respectively on the inoculated LB plates. After 36 h, the sizes of the inhibition zones around the filter papers were measured by vernier caliper. Broth dilution method was used to measure the minimum inhibitory concentrations (MICs) of glycine, Kocide 3000 and Gly-Cu(OH)<sub>2</sub> NPs.<sup>37</sup> The MIC was recorded as the lowest concentration at which no visible colonies grew after being inoculated at 28 °C for 72 h. All of the treatments were repeated four times in this experiment.

### Efficacy in greenhouse

To evaluate the antimicrobial activities of Kocide 3000 and Gly-Cu(OH)<sub>2</sub> NPs against the Xcc in greenhouse condition, Chinese cabbage (*Brassica rapa pekinensis*) was selected as a model plant and grown in plastic pots containing cultivated soil. After growing to a four-leaf stage, Gly-Cu(OH)<sub>2</sub> NPs at concentrations (0, 200, 400 and 800 mg L<sup>-1</sup> of copper) were sprayed onto the cabbage leaves. And the same concentrations of Kocide 3000 were used as the control. After treatments with the bactericides for 24 h, a bacterial suspension (3 × 10<sup>8</sup> CFU mL<sup>-1</sup>) was inoculated on the plants by spraying method. Each cabbage was covered with a transparent plastic bag. After 48 h, the bags were uncovered and all plants were placed in a greenhouse at 28 °C and ≥68% relative humidity. Then the disease index and



severity of black rot on Chinese cabbage were recorded at the 7th, and 14th days (grade 0: no infection; grade 1: 1–10% of leaves with wilt; grade 2: 11–25% of leaves with wilt; grade 3: 26–49% of leaves with wilt; grade 4: 50–74% of leaves with wilt; grade 5: whole leaves wilted). Each trial was repeated three times.

### Safety evaluation

Safety study of Gly-Cu(OH)<sub>2</sub> NPs was carried out to observe potential plant tissue damage. Studies were conducted using cabbage and tomato to compare their difference in oxidative stress tolerance levels. The seeds were sown in 7 × 7 cm flower pots containing artificial mixed soil composed of vermiculite and nutrient soil (1 : 4, v : v). After 21 days, the seedlings were sprayed with Kocide 3000, Gly-Cu(OH)<sub>2</sub> NPs at 200, 400, and 800 mg L<sup>-1</sup> of copper respectively. Glycine (400 mg L<sup>-1</sup>) and water were used as controls. The leaf SPAD value and the fresh weight were determined at 7 days after treatment, and then the fresh weight increase rates of plants treated with test compounds were calculated as follow formula:

$$\text{Fresh weight increase rate (\%)} = (W_t - W_c) / W_c \times 100$$

where  $W_t$  represents fresh weight treated with test compound and  $W_c$  represents control fresh weight. A chlorophyll meter SPAD-502 Plus (Konica Minolta, Inc., Osaka, Japan) was used to pinch five points on the leaf to record the leaf SPAD values. And then the seedlings (above ground) were washed, air-dried and weighed. Safety assessment was evaluated by a growth increase recorded as fresh weight and leaf SPAD value of the seedlings. All the treatments were repeated three times.

### Data analysis

All statistical analyses were conducted using SPSS 17.0 statistical analysis software (SPSS, Chicago, IL, USA). The data were analyzed by Duncan multiple range test ( $p < 0.05$ ) and expressed as the mean ± standard error of the mean (SEM) for all the experiments.

## Results and discussion

### Characterization of Gly-Cu(OH)<sub>2</sub> NPs

As shown in Fig. 1, the precursor complex *cis*-bis(glycinato)copper(II) monohydrate (*cis*-Cu(Gly)<sub>2</sub>·H<sub>2</sub>O) was prepared by mixing aqueous solution of copper(II) acetate and glycine at 70 °C. And then it was neutralized with sodium hydroxide

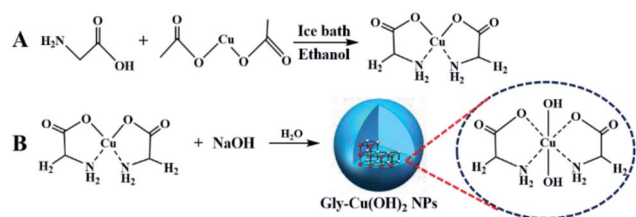


Fig. 1 Schematic preparation of Gly-Cu(OH)<sub>2</sub> NPs.

solution to synthesize Gly-Cu(OH)<sub>2</sub> NPs with blue color. The Gly-Cu(OH)<sub>2</sub> NPs could be stabilized in the water through ligand binding, which appears good water dispersibility. The copper content in Gly-Cu(OH)<sub>2</sub> NPs was 25.89 wt% by ICP-AES analysis.

The morphology and size of the as-prepared nanoparticles were confirmed by TEM. As shown in Fig. 2A, the mean diameter of Gly-Cu(OH)<sub>2</sub> NPs was approximately 230 nm. And the nanoparticles were aggregates of smaller sub-crystals with similar morphology and domain size (Fig. 2B). In order to determine the smaller subcrystals, HRTEM analysis was performed and displayed in Fig. 2C and D. The lattice fringe of smaller subcrystal was approximately 0.355 nm, which corresponded to the (111) lattice plane of Cu(OH)<sub>2</sub>. The mesocrystal Gly-Cu(OH)<sub>2</sub> NPs were stabilized by glycine surface ligands occluded between the individual nanoparticle domains.<sup>38</sup> EDS elemental mapping confirmed the presence of elements copper, nitrogen, oxygen, and carbon in the Gly-Cu(OH)<sub>2</sub> NPs (Fig. 2E). The copper content was similar to the result of the previous analysis by ICP-AES.

To further determine the differences between Cu(OH)<sub>2</sub> and Gly-Cu(OH)<sub>2</sub>, FTIR spectra, particle average size and zeta potential were analyzed. Compared with glycine, the *cis*-Cu(Gly)<sub>2</sub> (Fig. 3A-b) shows the characteristic vibration band of the carboxylic acid (–COOH) at 1523 cm<sup>-1</sup> disappears and the absorption band of the hydroxyl (–OH) at 676 cm<sup>-1</sup> appears a red shift owe to the coordination bond interference, which indicated that the synthesis of *cis*-Cu(Gly)<sub>2</sub> was successful. As shown in Fig. 3A-c, Cu(OH)<sub>2</sub> exhibits three strong characteristic peaks at 3570, 920, and 698 cm<sup>-1</sup>, which was assigned to the –OH stretching and vibrations. For the FTIR spectra of Gly-Cu(OH)<sub>2</sub> (Fig. 3A-d), the peaks at 1602 and 1326 cm<sup>-1</sup> are attributed to the stretching vibration of –COOH, and the band at 1390 cm<sup>-1</sup> is characteristic for the aliphatic C–H bonds in –CH<sub>2</sub> groups. Furthermore, in the region of 1100–1500 cm<sup>-1</sup>, two absorption peaks were detected due to the stretching of CH<sub>2</sub> and NH<sub>2</sub>. These changes in functional groups demonstrated the presence of glycine ligands in Gly-Cu(OH)<sub>2</sub> NPs. Particle size and zeta potential of Gly-Cu(OH)<sub>2</sub> NPs and Cu(OH)<sub>2</sub> measured by laser particle size analyzer are shown in Fig. 3B. The average size of Gly-Cu(OH)<sub>2</sub> NPs (240 nm) was significantly smaller than that of Cu(OH)<sub>2</sub> microparticles (2760 nm) because copper particles were embedded in glycine matrix to reduce particle

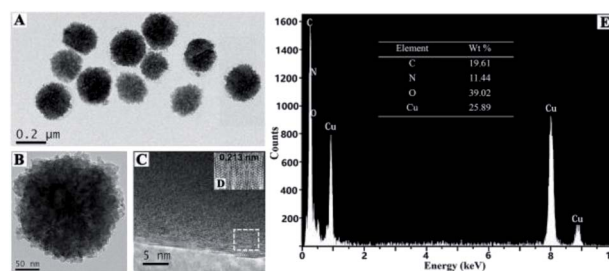


Fig. 2 TEM images of Gly-Cu(OH)<sub>2</sub> NPs synthesized from Cu(Gly)<sub>2</sub> (A and B). HRTEM image of (C) the edge of Gly-Cu(OH)<sub>2</sub> nanoparticle and (D) some individual Cu(OH)<sub>2</sub> NPs (crystallites). EDS pattern of Gly-Cu(OH)<sub>2</sub> NPs (E).



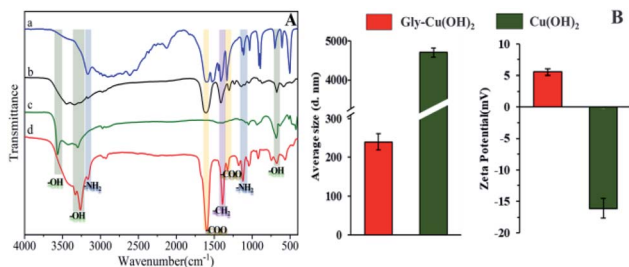


Fig. 3 (A) FTIR spectra of (a) glycine, (b) *cis*-Cu(Gly)<sub>2</sub>, (c) Cu(OH)<sub>2</sub>, (d) Gly-Cu(OH)<sub>2</sub>. (B) Particle average size and zeta potential of Cu(OH)<sub>2</sub> microparticles and Gly-Cu(OH)<sub>2</sub> NPs. The bars in the figure represent standard deviation ( $\pm$ SD).

aggregation. There was negative charges ( $-16.1$  mV) on surface of Cu(OH)<sub>2</sub> microparticles, while the surface of Gly-Cu(OH)<sub>2</sub> NPs has positive charges ( $+5.51$  mV), which meant that glycine was chelated with copper successfully in Gly-Cu(OH)<sub>2</sub> NPs.

### Antimicrobial assays *in vitro*

The antimicrobial properties of glycine, Kocide 3000, and Gly-Cu(OH)<sub>2</sub> NPs against *Xcc* strains were measured by the disk diffusion method. As shown in Fig. 4A, the diameters of the inhibition zone for Kocide 3000 and Gly-Cu(OH)<sub>2</sub> NPs (400 mg L<sup>-1</sup> of copper) were  $16.1 \pm 0.3$  mm and  $20.1 \pm 0.9$  mm, respectively.

But the *Xcc* strains had a rapid growth after treatment with glycine and no inhibitory zone was observed around the filter paper. The results clearly showed that the Gly-Cu(OH)<sub>2</sub> NPs had a better antimicrobial activity than Kocide 3000.

As shown in Fig. 4B, the density of bacteria decreased in a typical dose-dependent manner for the Kocide 3000 and Gly-Cu(OH)<sub>2</sub> NPs treatments. The growth of *Xcc* was completely inhibited by Gly-Cu(OH)<sub>2</sub> NPs when the concentrations were higher than  $100$  mg L<sup>-1</sup>, while the concentration of Kocide 3000 achieved the same efficacy was  $200$  mg L<sup>-1</sup>. The MIC of Gly-Cu(OH)<sub>2</sub> NPs was much less than that of Kocide 3000, indicating the prepared Gly-Cu(OH)<sub>2</sub> NPs had outstanding antimicrobial properties.

### Efficacy in greenhouse

As shown in Fig. 5, Gly-Cu(OH)<sub>2</sub> NPs and Kocide 3000 could significantly reduce the severity of black rot disease compared to the control at 7th day after spraying (control efficacy > 74.5%).

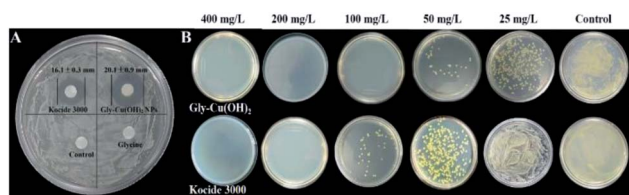


Fig. 4 (A) Inhibitory zone pattern of glycine, Kocide 3000, and Gly-Cu(OH)<sub>2</sub> NPs against *Xcc*. (B) Minimum inhibitory concentration of Gly-Cu(OH)<sub>2</sub> NPs and Kocide 3000.

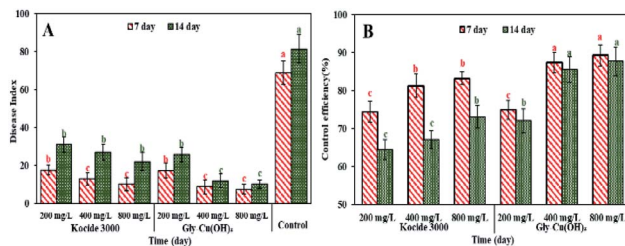


Fig. 5 The disease index (A) control efficiency (B) of black rot on Chinese cabbage seedlings treated with Kocide 3000 and Gly-Cu(OH)<sub>2</sub> NPs.

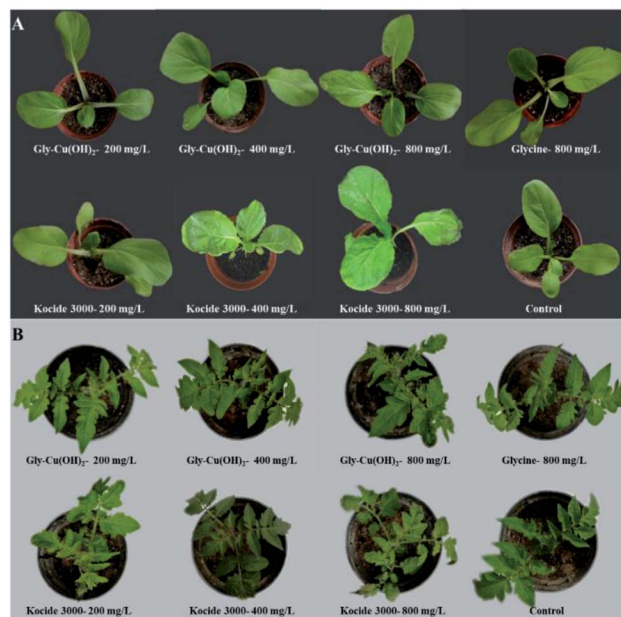


Fig. 6 The safety of Gly-Cu(OH)<sub>2</sub> NPs to Chinese cabbage (A) and tomato (B) seedlings.

There were significant differences between Gly-Cu(OH)<sub>2</sub> NPs and Kocide 3000 at concentrations of 400 and 800 mg L<sup>-1</sup> of copper, indicating the Gly-Cu(OH)<sub>2</sub> NPs could achieve better efficacy against *Xcc* than Kocide 3000 at medium and high concentrations. As mesocrystals, the Gly-Cu(OH)<sub>2</sub> NPs could be stabilized by glycine surface ligands occluded between the individual nanoparticle domains.<sup>35</sup> When copper hydroxide particles were embedded into the glycine, aggregation was prevented. Therefore, the Gly showed desirable biological activity due to better water dispersion and higher penetration ability through cell membranes of pathogenic bacteria than Kocide 3000.<sup>39–41</sup> After treatment for 14 days, Gly-Cu(OH)<sub>2</sub> NPs exhibited longer effective periods and better residual activities than Kocide 3000 at the same concentrations, which might attribute to the slow breaking of chelating bonds prevented the release of copper ions. In this work, the results were consistent with the previous researches which demonstrated that nano-meter-sized copper-based microbicides were more effective than the registered commercially copper-based products Kocide 2000 and Kocide Opti.<sup>42–44</sup> The possible antimicrobial



Table 1 The fresh weights and leaf SPADs of Chinese cabbage and tomato treated by Gly-Cu(OH)<sub>2</sub> NPs<sup>a</sup>

Treatment	Dosage (mg L <sup>-1</sup> )	Chinese cabbage seedling			Tomato seedling		
		Fresh weight (g)	Fresh weight increase rate (%)	Leaf SPAD value	Fresh weight (g)	Fresh weight increase rate (%)	Leaf SPAD value
Gly-Cu(OH) <sub>2</sub> NPs	200	6.17 ± 0.22	0.33ab	29.50 ± 2.51bc	2.31 ± 0.04	0.43ab	29.74 ± 1.21b
	400	6.19 ± 0.29	0.65ab	32.98 ± 1.53ab	2.37 ± 0.06	3.45a	32.58 ± 1.12a
	800	6.54 ± 0.14	6.34a	36.25 ± 3.05a	2.38 ± 0.05	3.88a	31.13 ± 1.25a
Kocide 3000	200	6.14 ± 0.26	0.33ab	28.35 ± 4.69bc	2.30 ± 0.04	0.31ab	29.65 ± 1.21b
	400	6.15 ± 0.26	0.16ab	26.26 ± 0.90c	2.28 ± 0.05	-0.48ab	29.84 ± 1.13b
	800	5.99 ± 0.13	-2.60b	26.23 ± 2.37c	2.19 ± 0.04	-4.41b	26.73 ± 1.46c
Glycine	800	6.48 ± 0.18	5.37a	31.53 ± 4.83ab	2.34 ± 0.05	2.14a	31.53 ± 4.83ab
Control	—	6.15 ± 0.24	—	30.06 ± 3.04bc	2.29 ± 0.04	—	29.58 ± 1.18b

<sup>a</sup> Mean values of fresh weight and leaf SPAD within each column followed by same letters are not significantly different at  $p < 0.05$ ,  $n = 5$ .

mechanism of Gly-Cu(OH)<sub>2</sub> NPs might be explained that the positively charged nanoparticles could be absorbed on the surface of the negative charged bacterial cells by electrostatic forces,<sup>45–47</sup> and the Cu ions released from Gly-Cu(OH)<sub>2</sub> NPs would act with protein of bacterial.<sup>48,49</sup>

### Safety evaluation

Fig. 6 showed the safeties of Gly-Cu(OH)<sub>2</sub> NPs to Chinese cabbage and tomato at the concentrations of 200, 400, and 800 mg L<sup>-1</sup> of copper. There was no any negative effect of Gly-Cu(OH)<sub>2</sub> NPs observed in Chinese cabbage (Fig. 6A). And the values of the fresh weight and SPAD treated with Gly-Cu(OH)<sub>2</sub> NPs (400 and 800 mg L<sup>-1</sup>) were higher than that of Kocide 3000 treatments at the same concentration. While there were some white spots observed on the Chinese cabbage leaves with treatment of high concentration of Kocide 3000 (800 mg L<sup>-1</sup>) (Fig. 6B).

The fresh weights of Chinese cabbage and tomato seedlings were increased respectively by 0.33–6.34%, 0.43–3.88% with treatments of Gly-Cu(OH)<sub>2</sub> NPs at the concentrations of 200, 400, and 800 mg L<sup>-1</sup> (Table 1). While Kocide 3000 showed the growth inhibition to tomato seedlings at the concentrations of 200, 400, and 800 mg L<sup>-1</sup> (Table 1). In particular, the growth inhibition rate of tomato seedlings reached up to 4.41% after Kocide 3000 treatment at a high concentration of 800 mg L<sup>-1</sup>. This could be attributed to the differences between Chinese cabbage and tomato seedlings in tolerance to copper, and glycine has a certain detoxification function in plants and could provide amino acid nutrition.<sup>50</sup> Thus, Gly-Cu(OH)<sub>2</sub> NPs were safe to plants and would be a potential alternative for sustainable crop protection.

## Conclusions

In this work, Gly-Cu(OH)<sub>2</sub> NPs were prepared by binding copper with glycine in sodium hydroxide solution. The ICP-AES, FTIR, HRTEM, and DLS analysis were used to characterize the prepared products. The results indicated that Gly-Cu(OH)<sub>2</sub> NPs had 25.89% (w/w) of copper content and showed good antimicrobial activity against *Xcc in vitro*. The greenhouse experiments

showed that Gly-Cu(OH)<sub>2</sub> NPs could significantly reduce the severity of black rot compared to the Kocide 3000. In addition, the prepared nanoparticles did not exhibit any phytotoxicity to plants and increased the fresh weights of Chinese cabbage and tomato seedlings by 6.34% and 3.88% respectively at the concentrations of 800 mg L<sup>-1</sup> of copper. Therefore, Gly-Cu(OH)<sub>2</sub> NPs with desirable antimicrobial activity and safety to plants have great potential for sustainable crop protection.

## Conflicts of interest

The authors declare no competing financial interest.

## Acknowledgements

This work was supported by the National and Local Joint Engineering Laboratory of High Efficiency and Superior-Quality Cultivation and Fruit Deep Processing Technology of Characteristic Fruit Trees in South Xinjiang (FE201801), Xinjiang Production & Construction Corps Key Laboratory of Protection and Utilization of Biological Resources in Tarim Basin (BRZD1903).

## References

- P. H. Williams, *Plant Dis.*, 1980, **64**, 736–742.
- J. G. Vicente and E. B. Holub, *Mol. Plant Pathol.*, 2013, **14**, 2–18.
- M. T. Islam, B.-R. Lee, V. H. La, H. Lee, W.-J. Jung, D.-W. Bae and T.-H. Kim, *Physiol. Mol. Plant Pathol.*, 2019, **106**, 270–275.
- D. Zhao, T. Mao, N. Wang, X. Zhao, X. Lou and G. Tao, *J. South. Agric.*, 2019, **50**, 761–767.
- R. E. Stall, *Plant Dis. Rep.*, 1962, **46**, 389–392.
- G. M. Marco and R. E. Stall, *Plant Dis.*, 1983, **67**, 779–781.
- E. G. Wulff, C. M. Mguni, C. N. Mortensen, C. L. Keswani and J. Hockenhull, *Eur. J. Plant Pathol.*, 2002, **108**, 317–325.
- S. Mishra and N. K. Arora, *World J. Microbiol. Biotechnol.*, 2012, **28**, 693–702.



- 9 G. A. Achari and R. Ramesh, *Proc. Natl. Acad. Sci., India, Sect. B*, 2019, **89**, 585–593.
- 10 A. Sessitsch, N. Pfaffenbichler and B. Mitter, *Trends Plant Sci.*, 2019, **24**, 194–198.
- 11 S. K. Sehmi, S. Noimark, J. Weiner, E. Allan, A. J. MacRobert and I. P. Parkin, *ACS Appl. Mater. Interfaces*, 2015, **7**, 22807–22813.
- 12 S. Dahiya, N. K. Mogha, K. Chaudhary, G. Kumar and D. T. Masram, *ACS Omega*, 2018, **3**, 16377–16385.
- 13 L. La Pera, G. Dugo, R. Rando, G. Di Bella, R. Maisano and F. Salvo, *Food Addit. Contam., Part A*, 2008, **25**, 302–313.
- 14 L. Zhang, J. Wang, G.-N. Zhu and L. Su, *Exp. Toxicol. Pathol.*, 2010, **62**, 163–169.
- 15 A. S. Adeleye, J. R. Conway, T. Perez, P. Rutten and A. A. Keller, *Environ. Sci. Technol.*, 2014, **48**, 12561–12568.
- 16 J. R. Lamichhane, E. Osdaghi, F. Behlau, J. Köhl, J. B. Jones and J.-N. Aubertot, *Agron. Sustainable Dev.*, 2018, **38**, 28.
- 17 A. Shrivastava, *Indian J. Environ. Prot.*, 2009, **29**, 552–560.
- 18 P. C. Nagajyoti, K. D. Lee and T. V. M. Sreekanth, *Environ. Chem. Lett.*, 2010, **8**, 199–216.
- 19 C. Ric de Vos, W. Ten Bookum, R. Vooijs, H. Schat and L. De Kok, *Plant Physiol. Biochem.*, 1993, **31**, 151–158.
- 20 N. Llorens, L. Arola, C. Bladé and A. Mas, *Plant Sci.*, 2000, **160**, 159–163.
- 21 I. Hoyle, B. J. Shaw and R. D. Handy, *Aquat. Toxicol.*, 2007, **83**, 62–72.
- 22 F. Gülser and E. Erdoğan, *Environ. Monit. Assess.*, 2008, **145**, 127–133.
- 23 Y. Liang, D. Yang and J. Cui, *New J. Chem.*, 2017, **41**, 13692–13699.
- 24 N. Horzum, M. E. Hilal and T. Isik, *New J. Chem.*, 2018, **42**, 11831–11838.
- 25 M. Maiti, M. Sarkar, S. Maiti and D. Liu, *New J. Chem.*, 2019, **43**, 662–674.
- 26 M. Young and S. Santra, *J. Agric. Food Chem.*, 2014, **62**, 6043–6052.
- 27 S. Zhang, N. Gao, T. Shen, Y. Yang, B. Gao, Y. C. Li and Y. Wan, *J. Mater. Chem. A*, 2019, **7**, 9503–9509.
- 28 P. Pulkkinen, J. Shan, K. Leppänen, A. Känkäkoski, A. Laiho, M. Järn and H. Tenhu, *ACS Appl. Mater. Interfaces*, 2009, **1**, 519–525.
- 29 U. Bogdanović, V. Lazić, V. Vodnik, M. Budimir, Z. Marković and S. Dimitrijević, *Mater. Lett.*, 2014, **128**, 75–78.
- 30 Y. Zhang, P. Zhu, G. Li, W. Wang, L. Chen, D. D. Lu, R. Sun, F. Zhou and C. Wong, *Nanoscale*, 2015, **7**, 13775–13783.
- 31 S. Pal, M. Das and K. Naskar, *Ind. Eng. Chem. Res.*, 2019, **58**, 17802–17813.
- 32 M. Pervaiz, I. Ahmad, M. Yousaf, S. Kirn, A. Munawar, Z. Saeed, A. Adnan, T. Gulzar, T. Kamal, A. Ahmad and A. Rashid, *Spectrochim. Acta, Part A*, 2019, **206**, 642–649.
- 33 W. Zhang, T. Shi, G. Ding, D. Punyapitak, J. Zhu, D. Guo, Z. Zhang, J. Li and Y. Cao, *ACS Sustainable Chem. Eng.*, 2017, **5**, 502–509.
- 34 A. M. Bukonjić, D. L. Tomović, A. S. Stanković, V. V. Jevtić, Z. R. Ratković, J. V. Bogojeski, J. Z. Milovanović, D. B. Đorđević, A. N. Arsenijević, M. Z. Milovanović, I. Potočnjak, S. R. Trifunović and G. P. Radić, *Transition Met. Chem.*, 2019, **44**, 65–76.
- 35 K. Korschelt, R. Ragg, C. S. Metzger, M. Kluncker, M. Oster, B. Barton, M. Panthöfer, D. Strand, U. Kolb, M. Mondeshki, S. Strand, J. Brieger, M. Nawaz Tahir and W. Tremel, *Nanoscale*, 2017, **9**, 3952–3960.
- 36 K. Fiebelkorn, S. Crawford, M. McElmeel and J. Jorgensen, *J. Clin. Microbiol.*, 2003, **41**, 4740–4744.
- 37 J. Cui, Y. Liang, D. Yang and Y. Liu, *Sci. Rep.*, 2016, **6**, 21423.
- 38 H. Fang, J. Lin, Z. Hu, H. Liu, Z. Tang, T. Shi and G. Liao, *Sens. Actuators, B*, 2020, **304**, 127313.
- 39 J. R. Conway, A. S. Adeleye, J. Gardea-Torresdey and A. A. Keller, *Environ. Sci. Technol.*, 2015, **49**, 2749–2756.
- 40 Y. Zhu, J. Xu, T. Lu, M. Zhang, M. Ke, Z. Fu, X. Pan and H. Qian, *Environ. Toxicol. Pharmacol.*, 2017, **56**, 43–49.
- 41 A. Strayer-Scherer, Y. Y. Liao, M. Young, L. Ritchie, G. E. Vallad, S. Santra, J. H. Freeman, D. Clark, J. B. Jones and M. L. Paret, *Phytopathology*, 2018, **108**, 196–205.
- 42 C. Gkanatsiou, K. Karamanoli, U. Menkissoglu-Spiroudi and C. Dendrinou-Samara, *Polyhedron*, 2019, **170**, 395–403.
- 43 W. Elmer and J. C. White, *Annu. Rev. Phytopathol.*, 2018, **56**, 111–133.
- 44 K. Giannousi, I. Avramidis and C. Dendrinou-Samara, *RSC Adv.*, 2013, **3**, 21743–21752.
- 45 J. S. Dickson and M. Koohmaraie, *Appl. Environ. Microbiol.*, 1989, **55**, 832–836.
- 46 M. Sugano, H. Morisaki, Y. Negishi, Y. Endo-Takahashi, H. Kuwata, T. Miyazaki and M. Yamamoto, *J. Liposome Res.*, 2016, **26**, 156–162.
- 47 J. H. Cui, Y. Liang, D. S. Yang and Y. L. Liu, *Sci. Rep.*, 2016, **6**, 10.
- 48 M. Perchlik and M. Tegeder, *Plant Physiol.*, 2018, **178**, 174–188.
- 49 H. S. Osman, *Ann. Agric. Sci.*, 2015, **60**, 389–402.
- 50 J. Niu, D. Guo, W. Zhang, J. Tang, G. Tang, J. Yang, W. Wang, H. Huo, N. Jiang and Y. Cao, *J. Hazard. Mater.*, 2018, **358**, 207–215.

